Environ Earth Sci (2016) 75:1388
DOI 10.1007/s12665-016-6209-x

ORIGINAL ARTICLE

The origin of high sulfate concentrations and hydrochemistry of the Upper Miocene–Pliocene–Quaternary aquifer complex of Jifarah Plain, NW Libya

Nawal Alfarrah[1,2] · Gebremedhin Berhane[1,3] · Ibrahimu Chikira Mjemah[1,4] · Marc Van Camp[1] · Kristine Walraevens[1]

Received: 1 May 2015 / Accepted: 14 October 2016 / Published online: 24 October 2016

Abstract The high uncontrolled groundwater extraction in Jifarah Plain, NW Libya, causes a modification of natural flow systems, inducing seawater intrusion and causing groundwater quality deterioration. The principal aim of this study is to identify the hydrogeochemical processes in this coastal aquifer in order to verify the main sources of sulfate concentration increase that occurs in the system. In order to achieve this aim, water samples were collected from 134 sampling wells in the study area and analyzed for the major cations and anions; physical and chemical parameters were measured, such as water level, electrical conductivity, pH and temperature. The analytical results obtained in the hydrochemical study were interpreted using Piper diagram, ion correlations with Na^+/Cl^-, SO_4^{2-}, Cl^- and TDS, in conjunction with calculation of the ionic deviations of the conservative freshwater/seawater mixture and saturation indices using the PHREEQC 2.16 software. The large SO_4^{2-} anomaly observed in groundwater near the coast was explained by the presence of seawater intrusion and upconing of deep saline water in these areas. This conclusion is based on high chloride concentrations, the inverse cation exchange reactions and the lower piezometric level compared to sea level. Inland, in Sabratah, the high SO_4^{2-} values are related to gypsum dissolution from the Upper Miocene Formation in the lower part of the upper aquifer. These locally high SO_4^{2-} concentrations in the south of the study area show overall increase in the upstream direction, which also suggests the dissolution of evaporites from the mountain aquifers in the south. High SO_4^{2-} concentration is also related to the effect of the scattered sebkha deposits in some areas along the coast.

Keywords Seawater intrusion · Overexploitation · Groundwater quality degradation · Gypsum dissolution · Sebkha · Upper aquifer · Tripoli

✉ Nawal Alfarrah
Nawalr2003@yahoo.com

Marc Van Camp
Marc.VanCamp@ugent.be

Kristine Walraevens
Kristine.Walraevens@ugent.be

[1] Laboratory for Applied Geology and Hydrogeology, Ghent University, Krijgslaan 281 S8, 9000 Ghent, Belgium

[2] Geology Department, Az Zawiyah University, Az Zawiyah, Libya

[3] Geology Department, Mekelle University, Mekelle, Ethiopia

[4] Department of Physical Sciences, Sokoine University of Agriculture (SUA), Morogoro, Tanzania

Introduction

The intrusion of seawater into coastal aquifers is a common problem in coastal zones of the world where increasing water requirements (Masciopinto et al. 1999) and arid climate have induced overexploitation of groundwater (Fidelibus and Tulipano 1992; Kreitler and Richter 1993; Park and Aral 2004; Van Camp et al. 2014). Continued exploitation of limited freshwater resources can also lead to up-flow of relict marine waters underlying the freshwater zone compounding the effects of seawater intrusion (Masciopinto 2006).

Next to admixture of seawater, the main sources of SO_4^{2-} in groundwater are oxidation of sulfide ores (pyrite FeS_2), and the dissolution of gypsum and anhydrite (Walraevens 1987; Coetsiers and Walraevens 2006, 2009; Coetsiers et al. 2009). Infiltration of industrial wastes can also add significant amounts of sulfate to freshwaters. Natural concentrations of SO_4^{2-} in freshwaters are usually less than 300 mg/l (Todd 1980).

The ever-growing demand for freshwater for a number of human purposes has become a worldwide cause of concern. Nowadays, groundwater reserves are exposed to intensive exploitation (Walraevens et al. 1994; Van Camp and Walraevens 2009; Van Camp et al. 2010, 2012, 2013), which may create serious problems in coastal areas where some hydraulic connection exists between the freshwater reservoirs and the sea (Masciopinto 2006; Mjemah et al. 2009; Van Camp et al. 2014; Walraevens et al. 2015).

Salinization is the most widespread form of groundwater contamination, especially in coastal aquifers, and is represented by the increase in total dissolved solids (TDS) and some specific chemical constituents such as Cl^-, Na^+, Mg^{2+} and SO_4^{2-} (Nadler et al. 1981; Magaritz and Luzier 1985; Dixon and Chiwell 1992; Bencini and Pranzini 1992; Bosch and Custodio 1992; Walraevens et al. 1993a, b; Morell et al. 1996; Sukhija et al. 1996; Chaouni Alia et al. 1997; Giménez and Morell 1997; Walraevens et al. 2007; Mtoni et al. 2012; Da'as and Walraevens 2013; Mtoni et al. 2013). The Jifarah Plain groundwater is affected by different sources of salinization, most serious is the seawater intrusion (Alfarrah 2011; Alfarrah et al. 2011).

Degradation of groundwater quality is usually thought of as the result of direct contamination of groundwater by either point source or diffuse source release of pollutants. In this study, results are presented of an investigation of declining water quality in a heavily dewatered aquifer system; seawater intrusion and water–rock interaction are responsible for the considerable variations in chemical composition of groundwater and for making it non-potable.

The origin of SO_4^{2-} may be traced through identification of hydrogeochemical processes. The aim of this study was to discover what processes have been responsible for variations in the chemical composition of groundwater in the upper aquifer of Jifarah Plain impacted by intense water withdrawal.

Study area

The study area covers the coastal part of the Jifarah Plain in NW of Libya (Fig. 1). The Jifarah Plain is a flat area of triangle shape of about 20,000 km^2. It is bordered by the Mediterranean Sea in the north, the Tunisian border in the West and Jebal Naffusah border in the south and east. The study area is a coastal strip of around 105 km length and 18 km wide in the north of central Jifarah, where more than 50 % of the country's population are concentrated. The climate of the region is semiarid, typically Mediterranean, with irregular annual rainfall; the average annual precipitation is around 250 mm. Jifarah coastal area, like all Mediterranean coastal regions, has experienced considerable periods of drought during the last two decades. The resulting water deficit was compensated through an increased withdrawal from aquifers.

The sediments of the Jifarah Plain have been deposited since early Mesozoic times in a near-shore lagoonal environment. Figure 1 represents the location and the general geological map for central Jifarah with the location of the main active pumping wells. The geological substratum, which is playing a role in the hydrogeology of the plain, comprises the Middle Triassic (Al Aziziyah Formation, consisting mainly of bedded limestone) and the Upper Triassic (Abu Shaybah Formation, consisting of continental sandstone). All post-Triassic formations have been eroded prior to the Miocene sedimentation. As a consequence, the Miocene, that covers about two-thirds of the coastal plain, overlays the Abu Shaybah deposits directly. An exception is found in some small down-faulted blocks southwest of Al Aziziyah area where the Lower Cretaceous Kiklah Sandstone and the Upper Cretaceous Ayn Tobi Limestone have been found in some locations.

Geological and hydrogeological setting

The principal aquifer used by the population in the Jifarah Plain is the Upper Miocene–Pliocene–Quaternary aquifer system, called "first aquifer" or "shallow aquifer" or "upper aquifer"; intercalated thin clayey sand and marl series are dividing the aquifer into a number of horizons, all are considered as one unconfined unit (Alfarrah et al. 2013). It is separated from the lower aquifers by Middle Miocene clay.

Table 1 gives a description of the Upper Miocene–Pliocene–Quaternary formations which are of most interest in the coastal area.

The upper aquifer is made up of a series of formations of uncertain age. Al Assah Formation is silt, sand and gravels with local occurrences of crystallized gypsum. The Pleistocene formations include terraces, which consist of cemented gravel and conglomerate. Qasr Al Haj Formation is mainly alluvial fans and cones consisting of clastic materials derived from the scarp. Jifarah Formation consists mainly of fine materials, mostly silt and sand, occasionally with gravel caliche bands and gypsum; it covers extensive parts of the Jifarah Plain. Gergaresh Formation, which is known as Gergaresh Sandstone of Tyrrhenian age, occasionally contains silt lenses and sandy limestone.

The Holocene deposits include recent wadi deposits; these deposits consist of loose gravels and loam. Beach sands are represented by a narrow strip at the coast and are made up of shell fragments with a small ratio of silica sands. Eolian deposits are represented by sand dunes and sheets covering large of the coastal strip (coastal dunes). These coastal dunes consist of shell fragments with small amounts of silica sands. It is worth mentioning that the

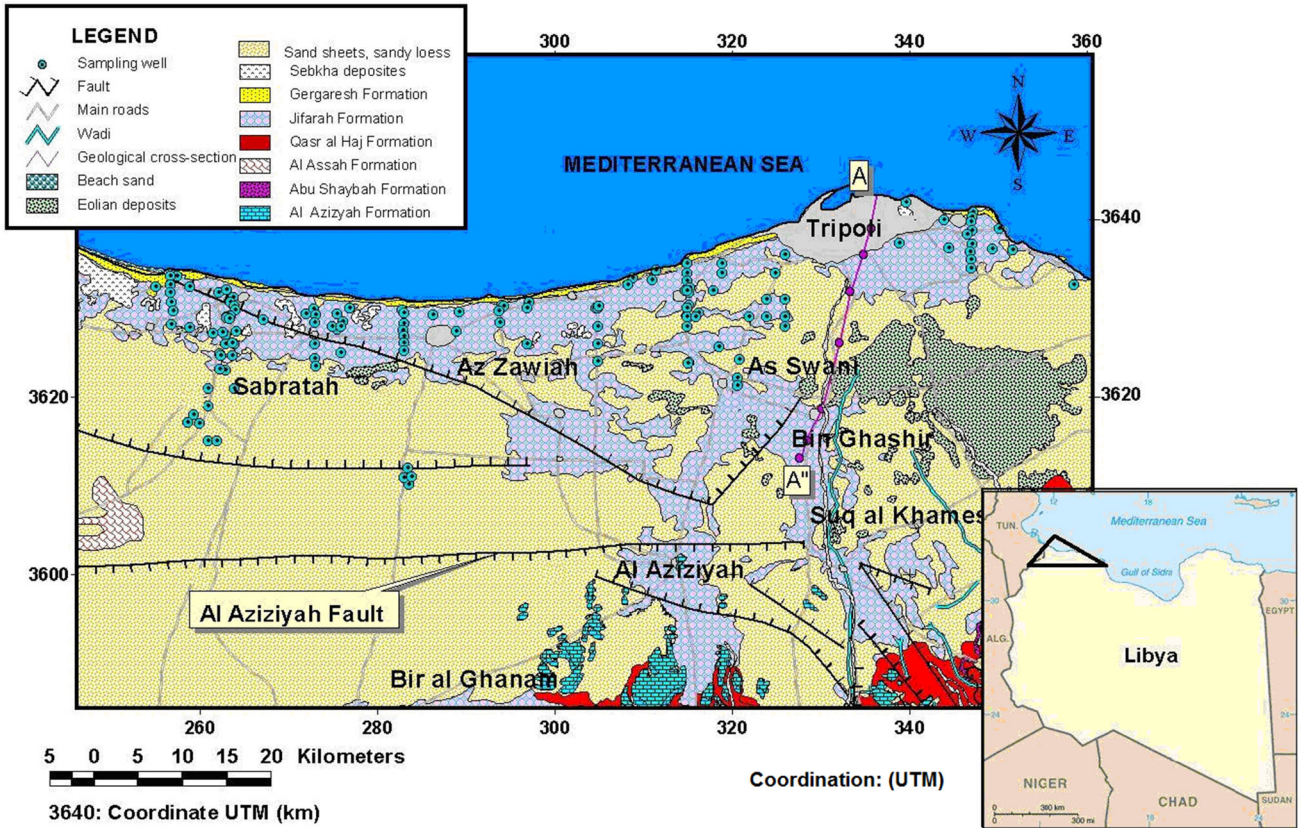

Fig. 1 Location and general geological map of the study area

Table 1 Description of the upper Miocene–Pliocene–Quaternary deposits in the coastal area of Jifarah Plain

Period	Epoch		Deposits and formations	Typical lithology	Thickness (m)
Quaternary	Holocene	Upper Miocene–Pliocene–Quaternary complex	Sand dunes and sand beach	Shale, silt, silica sand and gypsum	5–150
			fluvial–eolian deposits	Silt, clay, marl and fine sand	
			Sebkha	Sand, silt, clay and gypsum	
			Wadi deposits	Gravel, loam	
	Pleistocene		Gergaresh Formation	Conglomerate, sandstone, silt, sandy limestone	
			Jeffara Formation,	Alluvial cones and gravel	
			Qar al Haj Formation	Calcarenite	
Tertiary	Pliocene–Quaternary		Al Khums Formation	Limestone, dolomite	25–250
			Volcanic rocks	Basalt and phonolite	
	Miocene	Upper	Al Assah Formation	Silt, sand, gravel, limestone, gypsum	

eolian material composing coastal dunes contains a large amount of grains of gypsum. In some places, it is composed of nearly pure gypsum (98 %) especially in the immediate vicinity of the sebkhas, with a silty gypsum filling (LIRC 1995). Fluvial–eolian deposits are found on the plateau surface in central Jifarah. They are made up of silt, clay and fine sands with occasional caliche bands. Sebkha sediments are mainly gypsum deposits and observed along the coastal area of the plain. They occupy the relatively low topographic areas and are separated from the sea by sea cliffs. Some of the sebkhas have occasional incursions of the sea, and others may have subsurface connection with the seawater.

The depth to the bottom of the upper aquifer varies between 30 and 200 m and depths of the wells that are utilizing this aquifer are between 30 and 180 m. Most of the wells tapping this aquifer give productivity of about 20–80 m^3/h.

Methodology

Sampling and analytical methods

A regional hydrogeochemical survey and water level measurements were performed during dry periods from March to July in 2007 and from September to November of 2008. In the coastal area, a total of 134 shallow and deep wells (mostly 30–180 m deep), located at different distances from the Mediterranean Sea, were selected for groundwater sampling and water level measurement (see Fig. 1), along profiles perpendicular to the coastline. The samples were collected during pumping, and the water level measurements were performed in static condition.

The sampling points were chosen along vertical lines perpendicular to the coast, with lengths comprised between 8 and 28 km, in order to explore the aquifer from inland to the coast line. Water depth was measured from the ground surface using water level meter and was converted into water level by subtracting from ground elevation. The collected water samples were preserved in polyethylene bottles after filtering with 0.45-μm cellulose membrane filters. Two samples were taken from each well, one for determining anions and the other for determining cations. Samples for cation analysis were acidified to lower the pH to around pH = 2 by adding a few drops of nitric acid. Parameters measured are physical properties such as pH, temperature, water level and electrical conductivity. Cations (Na^+, K^+, Mn^{2+}, Fe^{Total}, Ca^{2+}, Mg^{2+}, Zn, Si) were analyzed using flame atomic absorption spectrometry (Varian). Anions (Cl^-, NO_3^-, NO_2^-, SO_4^{2-}, PO_4^{3-}) and NH_4^+ were analyzed using the molecular absorption spectrophotometer (Shimadzu). F^- was measured with ion selective electrode. Determination of bicarbonate (HCO_3^-) and carbonate (CO_3^{2-}) used the titration method with dilute HCl acid to pH 4.3 and 8.2, respectively. The above-mentioned analytical methods were used at the Laboratory of Applied Geology and Hydrogeology, Ghent University, and were provided in the Laboratory Manual and in Standard Methods for Examination of Water and Wastewater (APHA 1985). Careful quality controls were undertaken for all samples to obtain a reliable analytical dataset with an ionic balance error less than 5 %.

Hydrochemical evaluation methods

The interpretation process is mainly based on the calculation of the ion deviations (Δm_i) from conservative freshwater/seawater mixing, the calculation of the saturation indices (SI), graphical illustration methods including Piper diagram, calculation of ionic ratios, and elaboration of maps and cross sections showing the spatial and vertical distribution of water quality parameters in the study area.

Saturation indices

The PHREEQC 2.16 program was used to calculate saturation indices for calcite, dolomite, halite and gypsum based on the chemical analytical results and measured field temperatures for all samples.

Ion deviation from conservative freshwater/seawater mixing

Calculation of the ionic deltas Δm_i consists of a comparison of the actual concentration of each constituent with its theoretical concentration for a freshwater/seawater mix calculated from the Cl^- concentration of the sample (Fidelibus et al. 1993), because Cl^- is dominant ion in seawater and can be assumed to be conservative in many natural waters (Appelo and Postma 1993). The ionic deltas quantify the extent of chemical reactions, affecting groundwater composition, next to mixing. The chemical reactions during freshwater/seawater displacement can be deduced by calculating a composition based on the conservative mixing of seawater and freshwater, and comparing the conservative concentrations with those in the samples. The mass fraction of seawater (f_{sea}) in the groundwater can be obtained from chloride concentrations of seawater and freshwater as follows (Appelo and Postma 1993):

$$f\text{sea} = \frac{m_{Cl^-,\text{sample}} - m_{Cl^-,\text{fresh}}}{m_{Cl^-,\text{sea}} - m_{Cl^-,\text{fresh}}} \quad (1)$$

where $m_{Cl,\text{sample}}^{-}$ = the concentration of Cl^- in the sample expressed in mmol/l, $m_{Cl,\text{fresh}}^{-}$ = the concentration of Cl^- in the freshwater expressed in mmol/l, $m_{Cl,\text{sea}}^{-} = Cl^-$ concentration in the seawater end member in mmol/l ($Cl^- = 566$ mmol/l for mean ocean water; for Mediterranean seawater (possible end member), $m_{Cl,\text{sea}}^{-} = 645$ mmol/l).

Based on the conservative mixing of seawater and freshwater, the concentration of an ion i (m_i) in the mixed waters was calculated using the mass fraction of seawater f_{sea} as follows (Appelo and Postma 1993):

$$m_{i,\text{mix}} = f_{sea} \cdot m_{i,sea} + (1 - f_{sea}) \cdot m_{i,\text{fresh}} \quad (2)$$

where m_i is concentration of an ion i in mmol/l and subscripts mix, sea and fresh indicate the conservative mixture, and end members seawater and freshwater, respectively. Any change in concentration $m_{i,\text{reaction}}$ (Δm_i) as a result of reactions (not mixing) then becomes:

$$\Delta m_i = m_{i,\text{reaction}} = m_{i,\text{sample}} - m_{i,\text{mix}} \quad (3)$$

where $m_{i,\text{sample}}$ = the actually observed concentration in the sample in mmol/l.

The deviation from the conservative freshwater/seawater mixing is due to chemical reactions. A positive delta

means that the ion has been added to the water, e.g., due to desorption from the exchange complex. While adsorption will lead to negative delta.

Ions in infiltrating rainfall near the coast are often derived from sea spray, and only Ca^{2+} and HCO_3^- are added due to calcite dissolution (Appelo and Postma, 1993). All other ions are thus ascribed to seawater admixture. In this case, $m_{i,fresh} = 0$ for all components except Ca^{2+} and HCO_3^-.

The main end members used in the calculations for this study are the Mediterranean seawater and freshwater from the upper aquifer. For Mediterranean seawater where $Cl^- = 645$ mmol/l, the seawater fraction has been calculated as:

$$f_{sea} = \frac{m_{Cl^-,sample}}{645} \quad (4)$$

Table 2 shows the ion concentrations in standard seawater, Mediterranean seawater end member and the assumed freshwater end member in the Jifarah Plain. Recharge water in the plain is the water flowing to the aquifer from the high topographic recharge area in the south. As no data were collected from the south border of the plain, the groundwater in the recharge area is expected to have the same composition as the freshwater samples collected from a nearby high topographic region in Janzur, where the freshest water sample (*i.e.,* sample TJ17) is considered as a reference sample to the composition of freshwater coming from the south. The recharge water in sample TJ17 has a high concentration of Ca^{2+} and HCO_3^- as a result of calcite dissolution. The analyzed recharge water in the plain is also showing considerable concentrations of Na^+, Mg^{2+} and SO_4^{2-} as a result of carbonate and evaporite rocks dissolution in the unsaturated zone, and a greater impact of concentration by evaporation, that is characteristic for the study area.

Stuyfzand classification

The Stuyfzand classification (Stuyfzand 1986, 1992, 1993, 1999) subdivides the most important chemical water characteristics at 4 levels: the main type, type, subtype and class of a water sample (Table 3). Each of the four levels of subdivision contributes to the total code (and name) of the water type.

The *major type* is determined based on the chloride content, according to Table 3. The *type* is determined on the basis of an index for hardness (see Table 3), which can be expressed in French hardness degrees:

$$TH = 5 \times \left(Ca^{2+} + Mg^{2+}\right) \text{ in meq}/l.$$

The classification into *subtypes* is determined based on the dominant cations and anions. First the dominating hydrochemical family (and groups within families between brackets) is determined both for cations (Ca + Mg (Na + K) + NH_4 or (Al + H) + (Fe + Mn)) and anions (Cl, HCO_3 + CO_3 or SO_4 + (NO_3 + NO_2)). The most important cation and anion (group: within a group: the dominant ion in that group) determine the name of the subtype. Finally, the *class* is determined on the basis of the sum of Na^+, K^+ and Mg^{2+} in meq/l, corrected for a sea salt contribution (Eq. 5). This indicates whether cation exchange has taken place and also the nature of the

Table 2 Chemical composition of possible end members

Parameter (unit mg/l)	Analyzed recharge water in Jifarah Plain (sample: TJ17)	Standard seawater (Walraevens and Van Camp 2005)	Mediterranean seawater (Da'as and Walraevens 2010)
pH	7.97	8.2	–
Na^+	43.75	10,800	12,700
K^+	4.5	400	470
Ca^{2+}	49.51	410	470
Mg^{2+}	8.7	1290	1490
Cl^-	55.15	19,500	22,900
SO_4^{2-}	36.62	2690	3190
HCO_3^-	174.46	140	173
NO_3^-	29.1	0	0
NO_2^-	0.001	0.01	–
PO_4^{3-}	0.07	0.61	–
Fe (total)	0.008	3.4	–
Mn^{2+}	0.01	0.4	–
NH_4^+	0.001	1.16	–
SiO_2	–	6.2	–
TDS	401.88	35,242	41,393

Table 3 Water type classification (Stuyfzand 1986)

Main type	Code	Cl (mg/l)
Division in main types on the basis of chloride concentration		
Fresh	F	≤150
Fresh-brackish	Fb	150–300
Brackish	B	300–1000
Brackish-salt	Bs	1000–10,000
Salt	S	10,000–20,000
Hyperhaline	H	>20,000

Type		Code	Total hardness (mmol/l)	Natural occurrence in main types
Number	Name			
Subdivision of the main types on the basis of hardness				
−1	Very soft	*	0–0.5	F
0	Soft	0	0.5–1	F Fb B
1	Moderately hard	1	1–2	F Fb B Bs
2	Hard	2	2–4	F Fb B Bs
3	Very hard	3	4–8	F Fb B Bs
4	Extremely hard	4	8–16	Fb B Bs S
5	Extremely hard	5	16–32	Bs S H
6	Extremely hard	6	32–64	Bs S H
7	Extremely hard	7	64–128	S H
8	Extremely hard	8	128–256	H
9	Extremely hard	9	≥256	H

Class	Code	Condition (meq/l)
Subdivision of subtypes into classes according to $\{Na^+ + K^+ + Mg^{2+}\}$ corrected for sea salt		
$\{Na + K + Mg\}$ deficit	–	$\{Na + K + Mg\}$ corrected $< -\sqrt{0.5}\ Cl$
$\{Na + K + Mg\}$ equilibrium	0	$-\sqrt{0.5}\ Cl \le \{Na + K + Mg\}$ corrected $\le +\sqrt{0.5}\ Cl$
$\{Na + K + Mg\}$ surplus	+	$\{Na + K + Mg\}$ corrected $> \sqrt{0.5}\ Cl$

exchange, by assuming that all Cl^- originates from seawater, that fractionation of major constituents of the seawater upon spraying can be neglected and that Cl^- behaves conservatively.

$$\left\{Na^+ + K^+ + Mg^{2+}\right\}_{corrected} = \left[Na^+ + K^+ + Mg^{2+}\right] measured - 1.061 Cl^- \quad (5)$$

where − = often pointing at a saltwater intrusion; + = often pointing at a freshwater encroachment; and 0 = often pointing at an equilibrium.

A positive value greater than the error margin $\sqrt{0.50}$ Cl^- delivers "+" and refers to marine cation surplus, indicating freshening. A negative value ($<-\sqrt{0.50}$ Cl^-) delivers "−": marine cation deficit pointing to salinization. A value in between both negative and positive error margin delivers "0": equilibrium.

Each of the subdivisions contributes to the total code (and name) of the water type; for example B4-NaCl- reads as: "brackish extremely hard sodium chloride water, with a $\{Na^+ + K^+ + Mg^{2+}\}$ deficit." This deficit is often due to cation exchange during saltwater intrusion (salinization). It is well known that the hydrogeochemical composition of coastal groundwater affected by seawater intrusion is mainly controlled by cation exchange reactions next to the simple mixing process (Appelo and Postma 1993). These processes can explain deviations of the concentrations of cations from conservative mixing of both waters.

Results and discussion

Water level

The overexploitation of the Jifarah upper aquifer is characterized by the falling of piezometric head over a wide region, reducing the outflow rate to the sea, and the continuous degradation of the chemical quality of water. Depression cones in various places have dropped from 25 to 35 m below sea level (Fig. 2a), which testifies the inversion of the hydraulic gradient and the intrusion of seawater. This was mainly observed in Sabratah region and southern Tripoli.

Major hydrochemical parameters

Major anions and cations, pH, conductivity, total dissolved solids, as well as temperature, were assessed on all samples using WTW instrument. The results show that temperature ranges between 18 and 26 °C, pH range is 6.71–9.94, conductivity ranges between 510 and 15,650 µS/cm (25 °C), TDS range is 360–11,141 mg/l and chloride concentration ranges from 2 to 5285 mg/l. The high Cl^- concentration is due to mixing with seawater. High concentrations of chloride occur in all wells at a few kilometres from the coast, where the concentration of Cl^- increases downstream along the flow path. However, in many farther inland wells, it is still the dominant anion. Figure 2b shows a contour map with the spatial distribution of concentrations of Cl^- for the analyzed samples. Table 4 shows descriptive statistics for physico-chemical parameters of groundwater for selective representative samples in the Jifarah coastal area.

Figure 2c shows the spatial distribution of SO_4^{2-} for the analyzed samples. SO_4^{2-} concentration in the study area ranges from 27 to 2238 mg/l. Along the shoreline, the main source for increasing SO_4^{2-} is mixing with seawater, where seawater intrusion can add significant amounts of sulfate to freshwaters. This can be linked to the high Cl^- concentration in the upper aquifer along the coastal area,

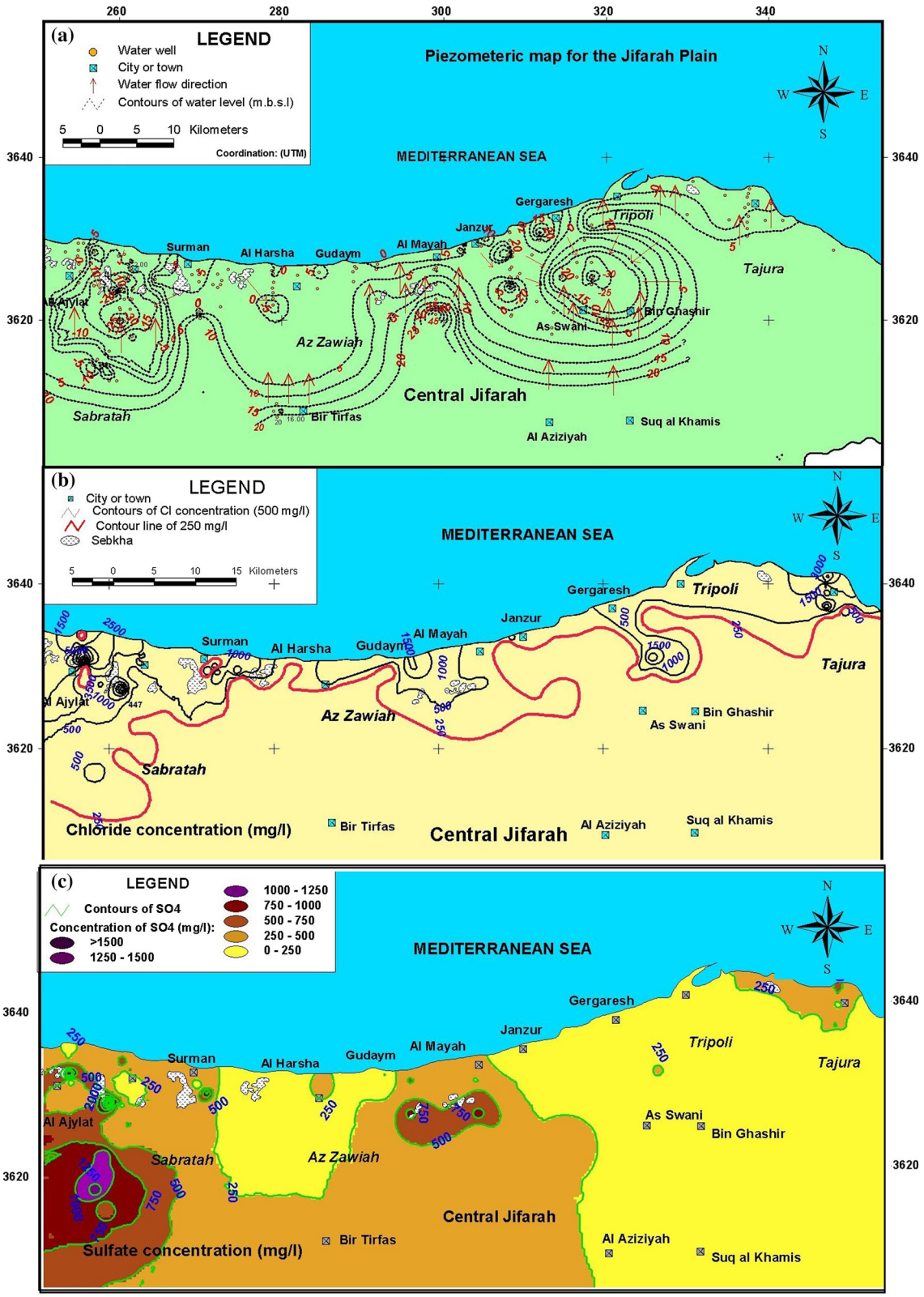

Fig. 2 **a** Piezometric map for the coastal area of central Jifarah. **b** The spatial distribution of Cl^- concentrations for the analyzed samples. **c** Spatial distribution of SO_4^{2-} in the upper aquifer

Table 4 Analytical results for physico-chemical parameters of groundwater for representative samples in the Jifarah coastal area

ID	Site	Ca^{2+} mg/l	Mg^{2+} mg/l	Na^{+} mg/l	K^{+} mg/l	$Fe^{2+/3+}$ mg/l	NO_3^{-} mg/l	HCO_3^{-} mg/l	Cl^{-} mg/l	SO_4^{2-} mg/l	pH	EC (μS/cm 25 °C)	T (°C)	Water level (m a.s.l)
A10	AL Ajylat	98.0	64.8	771	31.30	0.00	16.3	244	1092	452	7.30	4320	20	0.30
A4	AL Ajylat	652	252	1668	50.80	0.00	21.2	256	3949	548	7.65	11,960	25	2.00
A5	AL Ajylat	716	370	2749	74.30	0.00	19.9	360	5282	1547	7.88	15,650	24	2.00
S7	Sabratah	113	34.0	137	7.00	0.12	39.9	182	361	107	7.82	1500	20	−17.00
S8	Sabratah	85.9	24.0	109	7.00	0.17	45.9	175	195	96.5	7.63	1186	22	−17.00
S9	Sabratah	96.6	29.0	120	7.00	0.18	46.4	167	270	95.7	7.20	1412	23	−17.40
S10	Sabratah	112	50.4	133	11.70	0.00	13.8	153	316	178	7.90	1528	24	−25.00
S11	Sabratah	122	43.2	152	19.50	0.00	15.4	153	330	187	7.60	1627	24	−13.50
S19	Sabratah	339	125	219	8.00	0.18	98.2	196	319	1167	7.30	3250	21	−13.20
S22	Sabratah	782	228	389	11.00	0.27	77.5	183	864	2238	7.56	5380	21	−19.00
S23	Sabratah	401	128	207	8.00	0.06	136.2	180	224	1242	7.38	3430	21	12.00
SR4	Surman	224	80.4	189	11.70	0.00	23.2	189	560	331	7.89	2610	25	3.00
ZM40	Surman	554	76.8	676	23.50	0.00	6.6	153	2085	139	7.46	6530	24	3.50
ZM41	Surman	62.0	24.0	94.3	7.80	0.00	5.5	171	163	52.8	7.88	924	24	3.00
ZG1	Gudaym	346	51.6	538	11.70	0.00	16.7	305	1223	283	7.15	4550	24	1.00
ZG2	Gudaym	204	18.0	163	7.80	0.00	14.8	208	436	139	7.84	1930	24	5.00
TJ16	Janzur	77.6	46.6	64.0	4.00	0.00	77.5	220	89.9	160	7.86	1070	23	0.50
TJ17	Janzur	49.5	8.7	43.7	4.50	0.00	29.1	175	55.2	36.6	7.97	532	23	23.00
TG1	Gergaresh	117	91.0	206	4.00	0.09	60.6	284	441	117	7.75	2270	19	26.35
TG4	Gergaresh	116	28.3	156	9.00	0.38	55.5	199	247	135	7.78	1525	21	11.32
TG5	Gergaresh	121	51.3	114	4.00	0.68	78.8	196	302	43.5	7.15	1787	20	−6.25
TG6	Gergaresh	192	172.0	1023	22.00	0.16	76.5	232	1831	297	7.40	7660	22	−24.50
TG11	Gergaresh	47.2	28.6	66.1	3.00	0.11	36.5	224	99.1	63.2	7.71	798	22	−17.00
TG12	Gergaresh	85.6	55.0	107	5.00	0.17	34.0	273	141	215	7.59	1376	24	−41.50
TG13	As Suani	110	74.0	137	5.00	0.09	38.1	311	155	319	7.85	1761	24	−71.50
TG14	Gergaresh	103	80.0	130	6.00	0.17	68.3	258	242	260	7.21	1792	24	−65.50
TT2	Tajura	572	208.9	1129	70.40	0.00	0.80	421	2726	512	7.73	9150	22	0.00
TT6	Tajura	572	202.9	1178	19.50	0.00	23.2	226	3003	293	7.73	9310	21	0.00

where the highest concentrations were recorded to the west in Sabratah and in Tajura eastwards.

More than 1000 mg/l SO_4^{2-} is observed in the south of Sabratah region, at 11 km from the coast to about 18 km inland. The probable source of SO_4^{2-} is the dissolution of gypsum from the lower part of the upper aquifer, where gypsiferous sandstone and gypsiferous limestone are found in the formations that belong to the Upper Miocene, where low Cl^{-} is recorded, excluding seawater intrusion as the source. Increased seawater admixture increases SO_4^{2-} along the coast, where high Cl^{-} concentrations have been recorded.

Elsewhere, high concentrations over 1000 mg/l occur in the coastal area for several wells at the east of the study area in the area nearby Surman. In addition to mixing with seawater and/or upconing of deep saline water, the probable source of SO_4^{2-} for these wells is the dissolution of gypsum from the sebkha deposits in those areas, where these wells are located in the immediate vicinity of sebkha. The increase in SO_4^{2-} in the south of Sabratah is accompanied by an increase in NO_3^{-} concentrations. Part of the SO_4^{2-}-rich groundwater is derived from agricultural drainage water that flows through the sebkha deposits in Sabratah coast or through the lower part of the upper aquifer's sediments in the southern part, inducing dissolution of gypsum. Besides, the high SO_4^{2-} can be due to evaporation of highly concentrated irrigation water. High NO_3^{-} concentrations in these waters are a result of intensive agricultural activities in an area, which has been extensively irrigated during the last two decades (Alfarrah et al. 2011). Additional SO_4^{2-} might also add from the mountain aquifer as a significant amount of gypsum is present in its host rocks, which might contribute to the increase in SO_4^{2-} toward the south.

Out of 134 samples analyzed, 54 % have SO_4^{2-} higher than the highest desirable level of 200 mg/l (WHO 1993)

and 16 % have SO_4^{2-} higher than the maximum permissible value of 500 mg/l according to WHO (1993), with a maximum of 2238 mg/l for sample S22 south of Sabratah.

The dissolution of gypsum in groundwater found in several wells raises Ca^{2+} to significant levels up to 782 mg/l in groundwater. Further, next to the seawater intrusion and/or upconing of deep saline water, additionally, the dissolution of sebkha deposits (mainly consisting of gypsum) contributes to the increase in Ca^{2+} in several wells in the immediate vicinity of these deposits (*e.g.,* A23 with Ca^{2+} of 796 mg/l). Other wells, where sebkha deposits are playing a very important role in increasing the Ca^{2+} concentration, show concentrations between 200 and 652 mg/l. Further inland at more than 20 km south of Tripoli city, no data are available.

Water types and Piper diagram

Classification of hydrochemical facies for groundwaters according to the Piper diagram is represented in Fig. 3a, b.

In the Piper diagram, almost all water samples are plotted above the seawater–freshwater mixing line (comprising freshwater sample TJ17 and Mediterranean Sea water), due to Ca^{2+} surplus. Although various hydrochemical facies were observed (NaCl, CaCl, MgCl, $CaHCO_3$, $NaHCO_3$ and $CaSO_4$), CaCl and NaCl types are dominant. Large proportions of the groundwaters show NaCl type, which generally indicates a strong seawater influence (Pulido-Leboeuf 2004) or upconing of deep saltwater, while CaCl water type is indicating salinization and cation exchange reaction (Walraevens and Van Camp, 2005). The region of the CaCl type water may be a leading edge of the seawater plume (Vengosh et al. 1991; Appelo and Postma 1993; Jeen et al. 2001). Furthermore, sources of $CaSO_4$ water type are the dissolution of gypsum from the deeper parts of the aquifer and, to some extent, the dissolution of the scattered sebkha deposits.

Furthermore, in the south toward the recharge area and in the Janzur coast, groundwater of $NaHCO_3$ and $CaHCO_3$ type is associated with the lowest mineralization. This reflects the dissolution of carbonate minerals in carbonate aquifers which make up most of the watershed boundaries.

In the south of Janzur, $MgSO_4$ and $NaSO_4$ water types are observed for some samples, which might be due to upward flow from the lower aquifer, which has high sulfate content in this region (Alfarrah et al. 2011).

Hydrochemical profile

Salinization is induced as the new saline end member is introduced into the freshwater aquifer. The main chemical reaction is cation exchange, resulting in deficit of Na^+ and surplus of Ca^{2+}:

$$Na^+ + 0.5Ca - X_2 \rightarrow Na - X + 0.5Ca^{2+}$$

where X represents the natural exchanger in the reaction. During cation exchange, the dominant Na^+ ions are adsorbed and Ca^{2+} ions released, so that the resulting water moves from NaCl to CaCl water type, which is typical for salinization (Jones et al. 1999). The salinization process can be schematized as follows (Walraevens and Van Camp 2005):

$$CaHCO_30 \Rightarrow CaCl^- \Rightarrow NaCl- \Rightarrow NaCl0$$

F (fresh) $\Rightarrow$ Fb (fresh-brackish) $\Rightarrow$ B (brackish) $\Rightarrow$ Bs (brackish-saline) $\Rightarrow$ S (saline).

The chloride ion concentration is taken as a reference parameter (Jones et al. 1999). Therefore, as saltwater intrudes coastal freshwater aquifers, the Na/Cl ratio decreases and the Ca/Cl ratio increases.

Upon the inflow of freshwater a reverse process takes place:

$$0.5Ca^{2+} + Na - X \rightarrow 0.5Ca - X_2 + Na^+$$

Flushing of the saline aquifer by freshwater will thus result in uptake of Ca^{2+} by the exchanger with concomitant release of Na^+. This is reflected in the increase in the Na/Cl ratio, and formation of the $NaHCO_3$ water type, which is typical for freshening. The anion HCO_3^- is not affected because natural sediments behave as cation exchanger at the usual near-natural pH of groundwater (Appelo 1994). The freshening process can be schematized as follows (Walraevens and Van Camp 2005):

The hydrogeochemical profile in Sabratah (Fig. 4) is selected as an example showing the evolution of water salinity along the flow path. In this profile, the water type based on Stuyfzand (1986) is shown, including the specification of the Mix water type. The position of the names of the water types that are indicated above the water table has no relation with the sampling depth. In Sabratah, the waters are brackish and enriched with Cl^- and Ca^{2+}. The water types change from NaCl and CaCl in the north, to CaMix in the central zone and further to $CaSO_4$ southwards. Close to the shoreline, the water is NaCl type, due to strong effect of seawater. CaCl results from cation exchange, due to mixing with seawater. In the central zone (Suq al Alalqah), CaMix($ClHCO_3$) evolving further inland to CaMix(SO_4-Cl), indicates the location of the transition zone, where the groundwater changes from CaMix enriched with Cl^- ion to CaMix with SO_4^{2-} as the dominant anion. The $CaSO_4$ water type observed in the upstream zone to the south, up to 18 km inland, shows the existence of the evaporitic rocks intercalated within the sandstone layers of the aquifer.

The Mg^{2+} content found in all wells in the upstream zone is mainly resulting from the freshwater end member

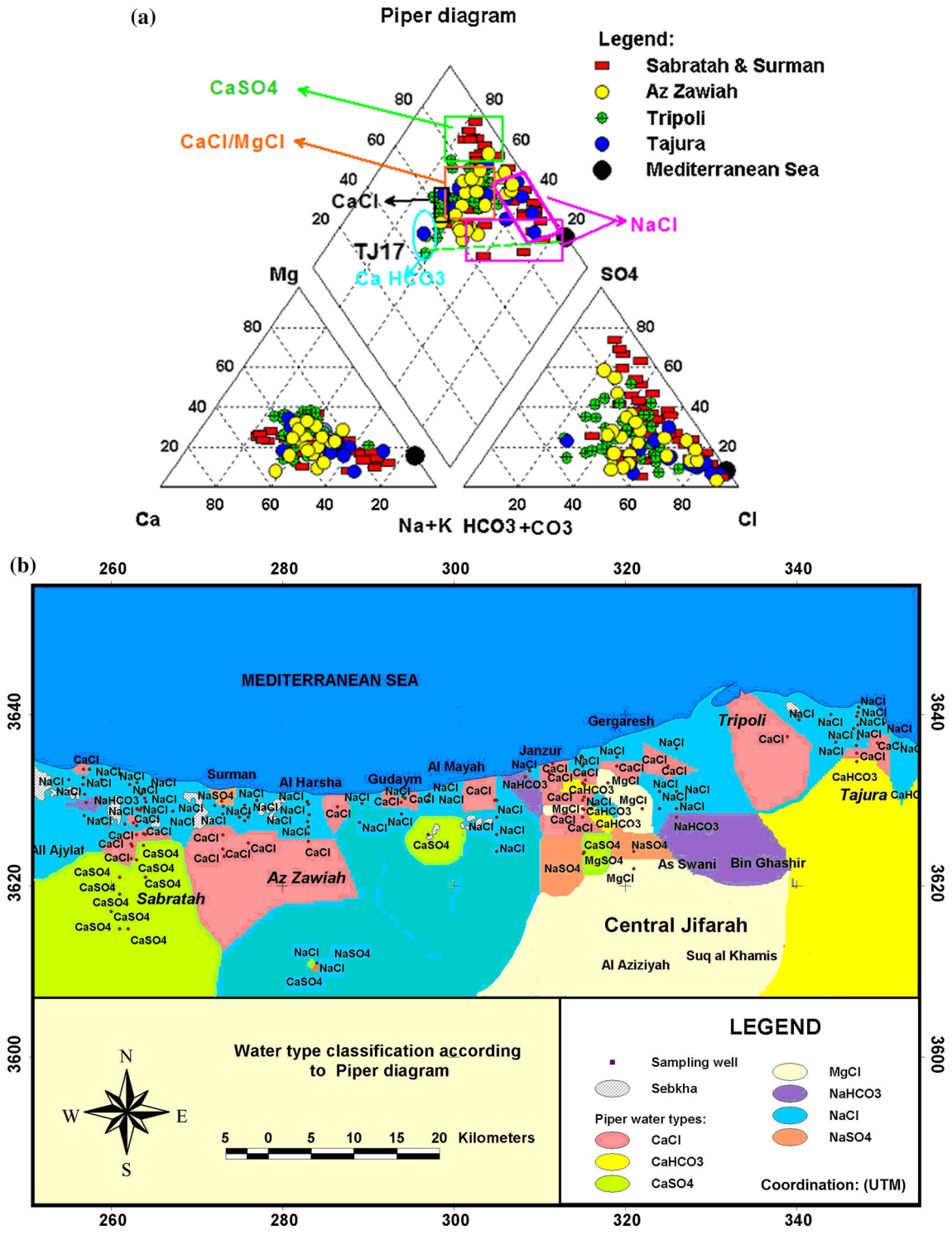

Fig. 3 **a** Water types according to Piper diagram. **b** Spatial distribution of water types according to piper diagram

coming from the recharge area, where Mg^{2+}-containing carbonate is dissolved (Alfarrah et al. 2011). The positive cation exchange code in the classification name is in this case thus not indicating freshening as Mg^{2+} is not supplied by the marine end member. From the central zone and downstream, cation exchange equilibrium (cation exchange code "0") exists for most of wells, which in this case indicates the onset of the salinization process $((Na^+ + K^+ + Mg^{2+})_{corrected}$ is decreasing as its cations are adsorbed). The water level is showing low heads, and the

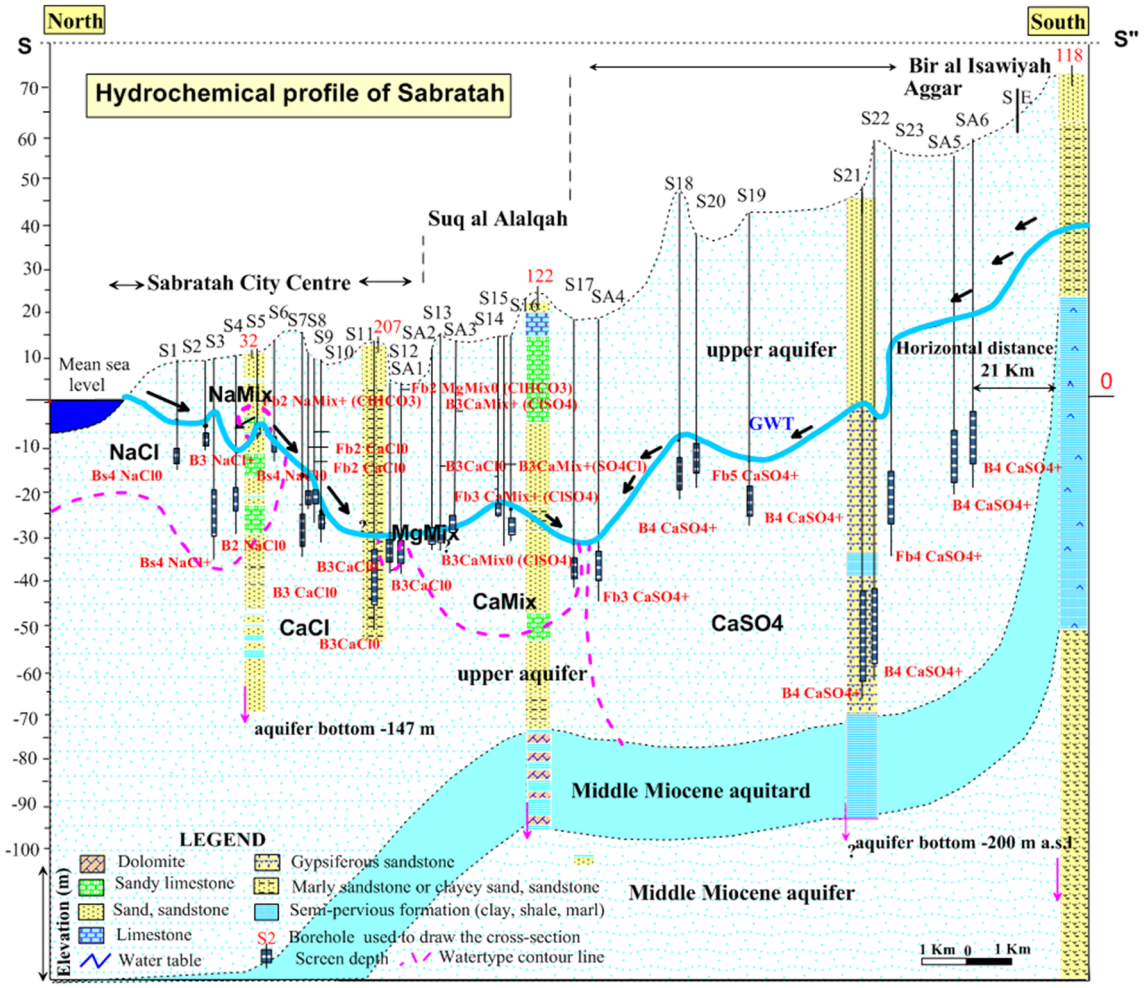

Fig. 4 Hydrochemical profile in Sabratah area (profile S–S")

EC remains above 1000 µS/cm (25 °C) in all wells, indicating a high level of salinity for the aquifer in this area.

The salinization in this area is mainly due to seawater intrusion and upconing of deep saline water (e.g, S3 & S5 in Fig. 4) in the downstream and central zones. Besides, the salinization may be linked to interaction between groundwater and gypsum in the upstream zone.

Saturation indices

The saturation indices (SI) for calcite, dolomite, halite, aragonite, gypsum and anhydrite were calculated to verify precipitation and dissolution of these minerals. The selected minerals were based on the major ions in groundwater from the study area. Figure 5 is a diagram showing SI values for calcite, dolomite, gypsum, anhydrite, halite and aragonite organized from west to east in the x axis. The sample numbers are sorted according to their location from west to east. The figure also represents an approximate location of samples for each area.

Out of 134 groundwater samples, 86 % of groundwaters seem to be supersaturated ($SI > 0$) in respect to calcite ($CaCO_3$), whereas 9 % are undersaturated in respect to calcite ($SI < 0$) and 5 % are at equilibrium ($SI = 0$). Dolomite ($MgCa(CO_3)_2$) seems to be oversaturated in 81 % of groundwater samples analyzed, 14 % are undersaturated and 5 % are at equilibrium. 98 % of groundwater samples in the study area are undersaturated in respect to gypsum ($CaSO_4{\cdot}2H_2O$) and anhydrite ($CaSO_4$).

In general most of the analyzed samples have saturation indices close to saturation in respect to calcite (SI mostly 0–1) and dolomite (SI mostly 0–2). This supersaturation with respect to calcite and dolomite rather points to water in equilibrium with those minerals. During sampling, most often dissolved CO_2 gas escapes, slightly raising pH and thus shifting carbonate equilibrium (more CO_3^{2-}), such that SI > 0 is obtained, whereas in water in the aquifer SI with respect to calcite is close to zero. So, the water is not really oversaturated, it just seems to be oversaturated or has some tendency to oversaturation.

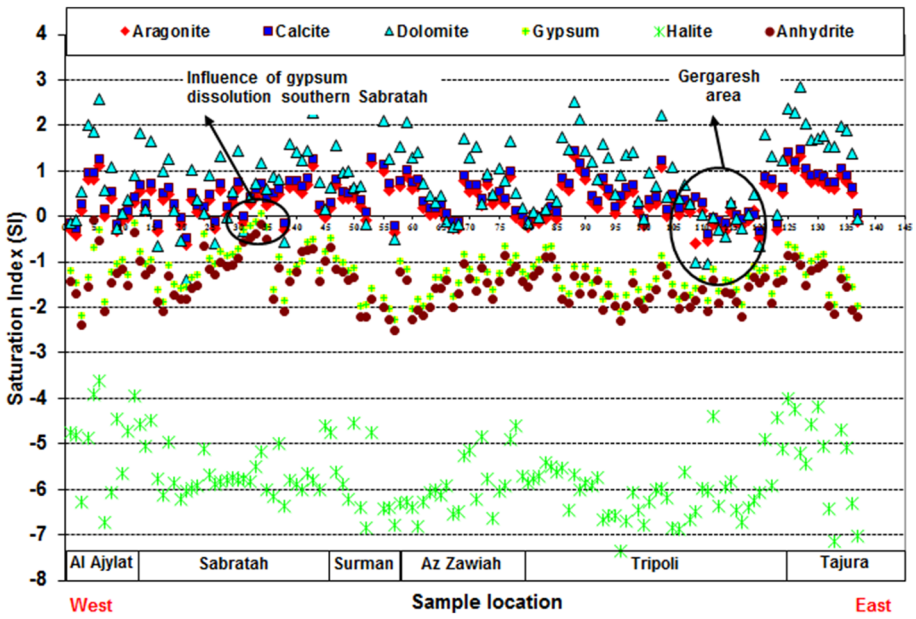

Fig. 5 Calculated saturation indices of groundwater samples with respect to selected minerals

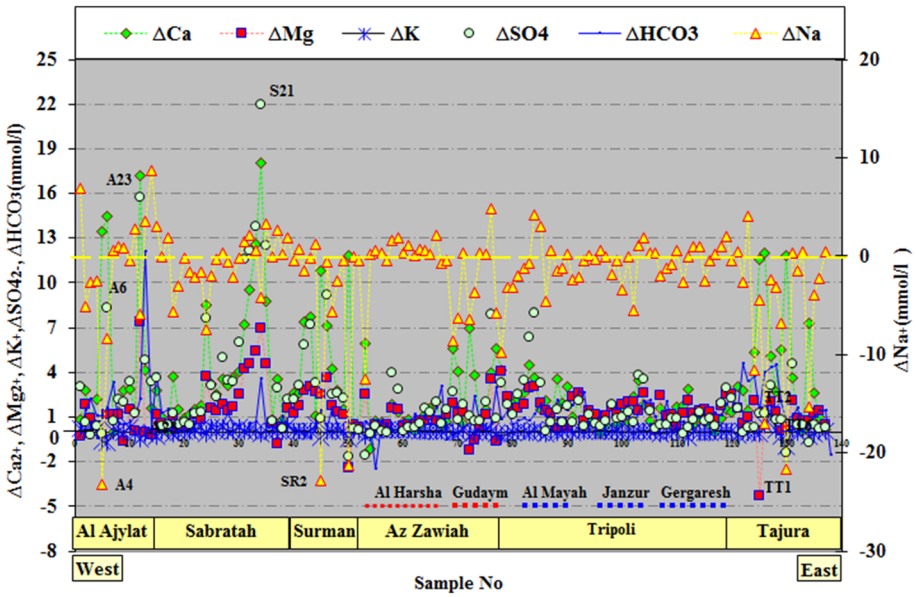

Fig. 6 Diagram of ionic delta for all analyzed samples

The majority of samples in the study area are undersaturated with respect to gypsum and anhydrite. Gypsum comes close to saturation (SI > -0.76) in many wells. The dissolution of gypsum from the deeper part of the aquifer and from superficial sebkha deposits for many wells in the coastal area raises the SI. In several samples at the south of Sabratah, groundwater was found to be saturated (for one sample) or close to saturation toward gypsum and anhydrite, where dissolution of gypsum from the upper aquifer influences the chemical groundwater composition. Other samples are close to the saturation indicating evaporite rocks dissolution from sebkha deposits. Hence, if gypsum is present, its dissolution will play a role in defining the groundwater composition, especially in systems with limited groundwater flow.

Deviation from conservative mixture of end member fraction

Figure 6 shows the ionic deltas calculated for Na^+, Ca^{2+}, Mg^{2+}, K^+, HCO_3^- and SO_4^{2-} for all analyzed samples. The first thing to note is that the processes in the mixing zone of this aquifer are complex and do not show a homogeneous pattern. For example, in Fig. 6 $m_{Na+,reaction}$ (ΔNa^+) is plotted in the secondary axis; the ΔNa^+ is usually positive for freshwater, but a large number of samples have

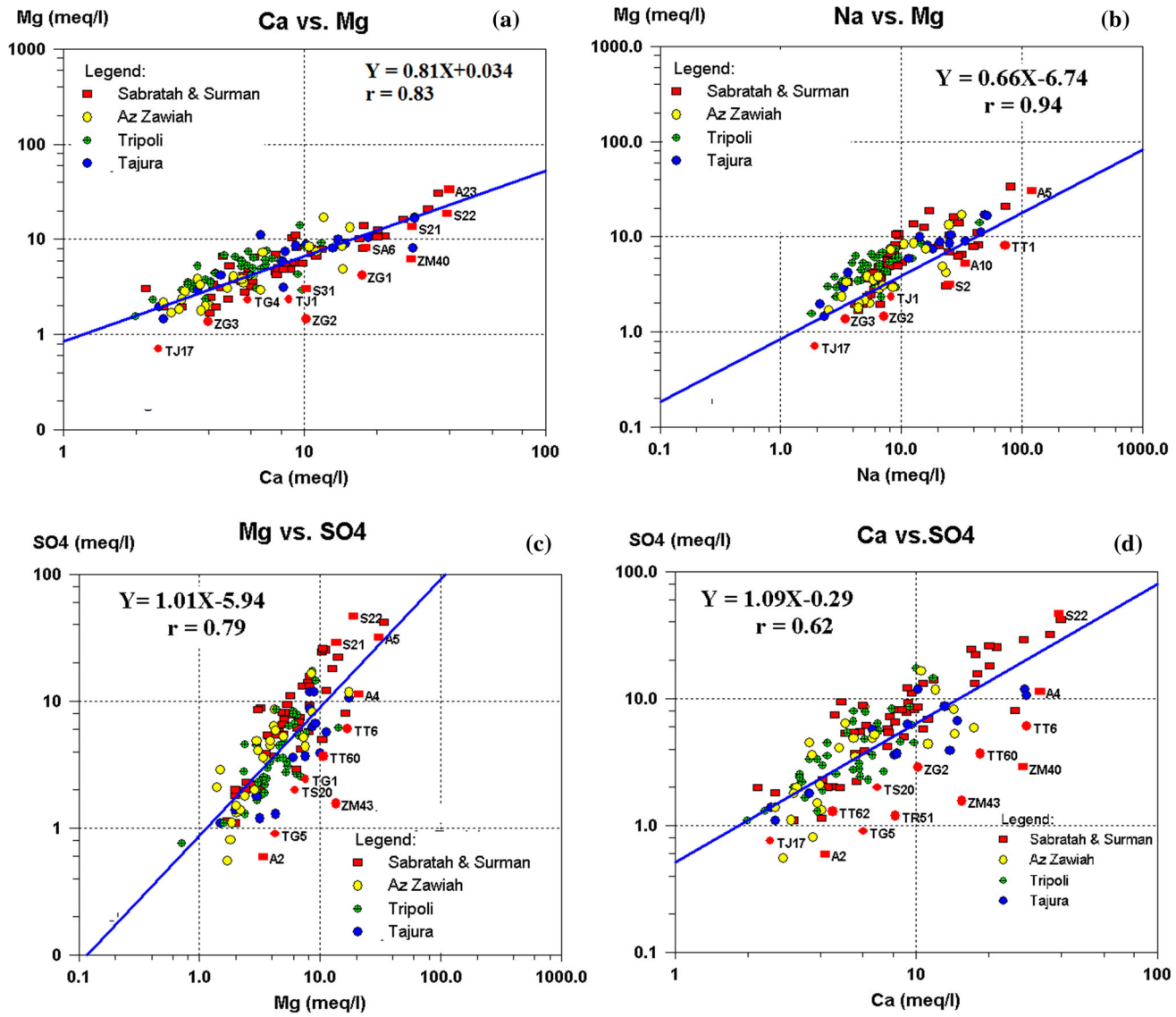

Fig. 7 Ca^{2+} versus Mg^{2+}, Na^{+} versus Mg^{2+}, Mg^{2+} versus SO_4^{2-} and Ca^{2+} versus SO_4^{2-}. The *lines* represent a linear regression

negative values particularly in the highly saline water, down to −24 mmol/l. The most logical explanation for this deficit of Na^{+} is that a reverse cation exchange reaction is taking place during the salinization processes, which releases Ca^{2+} to the solution and captures Na^{+}. A reverse relationship between the two ions (Na^{+} and Ca^{2+}) is noticed particularly in the highly saline groundwater, where samples with large negative values of ΔNa^{+} generally show strong positive ΔCa^{2+}. Furthermore, potassium shows negative or low positive deltas characteristic for marine cations as a result of the salinization process.

ΔMg^{2+} is mostly positive, due to more Mg^{2+} added by dissolution of Mg^{2+}-rich carbonate than adsorbed at the clay exchange complex during salinization. Only very few samples show a deficit of Mg^{2+}. Figure 6 also shows that the ionic delta of ΔHCO_3^{-} is close to zero or positive for most water samples. This fact suggests some dissolution of carbonate minerals in the aquifer deposits. In general, most samples show positive ΔSO_4^{2-}. Only a few samples show negative ionic delta of SO_4^{2-}, which indicates sulfate reduction. The gypsum dissolution increases ΔSO_4^{2-} to high positive values up to 22 mmol/l.

Dissolved ion ratios

Figure 7 shows scatter plots of Ca^{2+} vs Mg^{2+}, Na^{+} versus Mg^{2+}, Cl^{-} vs SO_4^{2-} and Ca^{2+} versus SO_4^{2-}. The upstream direction of the upper aquifer in Sabratah region is accompanied by a general increase in Ca^{2+}, Mg^{2+} and SO_4^{2-} (see Fig. 5), where sulfate and calcium become dominant. As mentioned above, in Sabratah area, the brackish extremely hard $CaSO_4$ type is frequently found

related to gypsum dissolution. The high salinity and relatively high concentrations of SO_4^{2-} found in some samples taken from inland wells can be related to this process. On the basis of currently available data, we cannot discard the possibility that additionally, a process of marine intrusion is affecting areas of the aquifer close to these points (south of Sabratah), where the concentration of Cl^- is relatively high for many wells.

From Fig. 7, it can be concluded that Ca^{2+} and Mg^{2+} correlate positively and significantly with SO_4^{2-} ($r = 0.62$ for Ca^{2+} and $r = 0.79$ for Mg^{2+}; Fig. 7d, c). The high correlation coefficient $r = 0.62$ between Ca^{2+} and SO_4^{2-} is related to the dissolution of gypsum from the lower part of the aquifer and from the superficial sebkha deposits in the region. A significant Mg^{2+} contribution is added from the intrusion of seawater next to some contribution from carbonate dissolution. Low positive correlation is found between Ca^{2+} and Mg^{2+} ($r = 0.37$, Fig. 7a), where the concentration of Ca^{2+} in seawater is much lower than Mg^{2+} and most of Ca^{2+} is derived from the dissolution of calcite in the freshwater aquifer. This is further reflected by the high correlation coefficient between Mg^{2+} and SO_4^{2-} ($r = 0.79$, Fig. 7c), and Mg^{2+} and Cl^- ($r = 0.95$). The lower concentration of Ca^{2+} compared to Na^+ close to the seaside and at the depression cones for some samples, is the result of strong seawater influence.

Also the high correlation coefficient for the scatter plot with the linear regression line of Na^+ versus Mg^{2+} ($r = 0.94$, Fig. 7b) is explained by marine intrusion.

Figure 8a, b shows scatter plots of TDS vs Cl^- and Cl^- versus SO_4^{2-}.

From Fig. 8a, less Cl^- in the mixture and the high TDS is explained due to the extra source of SO_4^{2-} coming from the dissolution of gypsum from the upper aquifer's formation in the southern study area. Furthermore, the scattered sebkha deposits produce high SO_4^{2-} waters for several wells.

Figures 9 and 10 show the ion ratio diagrams (Na^+/Cl^- versus Cl^- and SO_4^{2-}/Cl^- versus TDS) based on the analytical results shown in appendix 1.

Lower ratios of Na^+/Cl^- (meq l^{-1}/meq l^{-1}) than the Mediterranean seawater ratio (0.88, Fig. 9) indicate seawater encroachment, whereby Na^+ becomes adsorbed to sediment during the cation exchange reaction occurring when seawater intrudes freshwater aquifers, resulting in the deficit of Na^+ and surplus of Ca^{2+}. The Na^+/Cl^- ratios in the study area range from 0.38 to 1.68. Fifty-seven percent are lower than the Mediterranean seawater ratio, 74 % are lower than or slightly higher than the Mediterranean seawater ratio ($Na^+/Cl^- < 1$), whereas the other 26 % are clearly higher values. Toward the recharge area, the Na^+/Cl^- ratio is rising gradually, where it reaches more than 1.20 for some wells. Most of water samples in the downstream direction show low Na^+/Cl^- ratio, except samples from Janzur, where the Na^+/Cl^- ratio is more than 1.0. Very low (<0.88) ratios are recorded just few meters from the coast and in the depression cones.

Furthermore, to evaluate the effect of seawater mixing qualitatively, the ionic ratio SO_4^{2-}/Cl^- (mg l^{-1}/mg l^{-1}) has been examined versus TDS (Fig. 10).

There is a wide range of the SO_4^{2-}/Cl^- ratio versus TDS suggesting that the Jifarah Plain groundwater is controlled by other processes in addition to cation exchange during seawater mixing, where samples from the southwestern part of the coastal area of Sabratah and the ones collected at the immediate vicinity of sebkhas have a higher SO_4^{2-}/Cl^- ratio than the fresh recharge water ratio

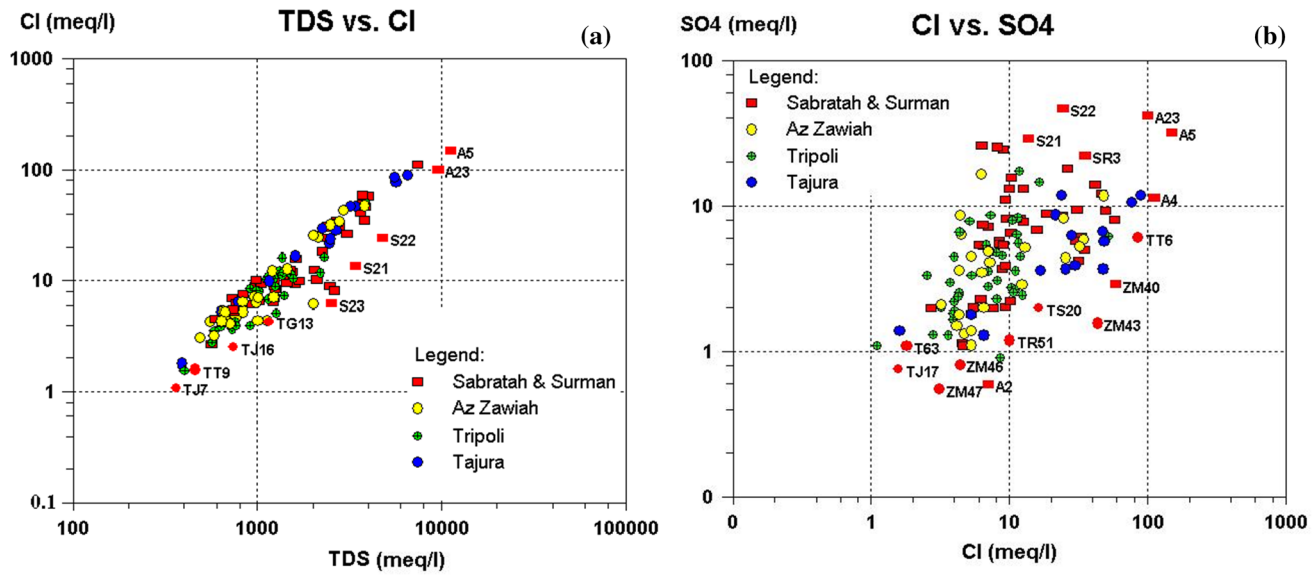

Fig. 8 TDS versus Cl^- and Cl^- versus SO_4^{2-}. The *lines* represent the mixing curve of recharge water and Mediterranean seawater

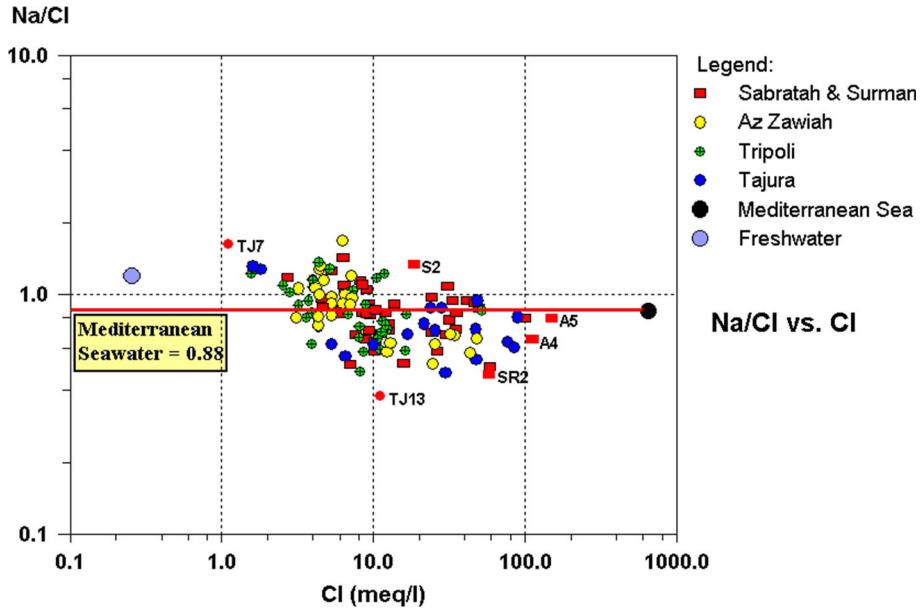

Fig. 9 Molar ratio of Na+/Cl^- versus Cl^- concentrations

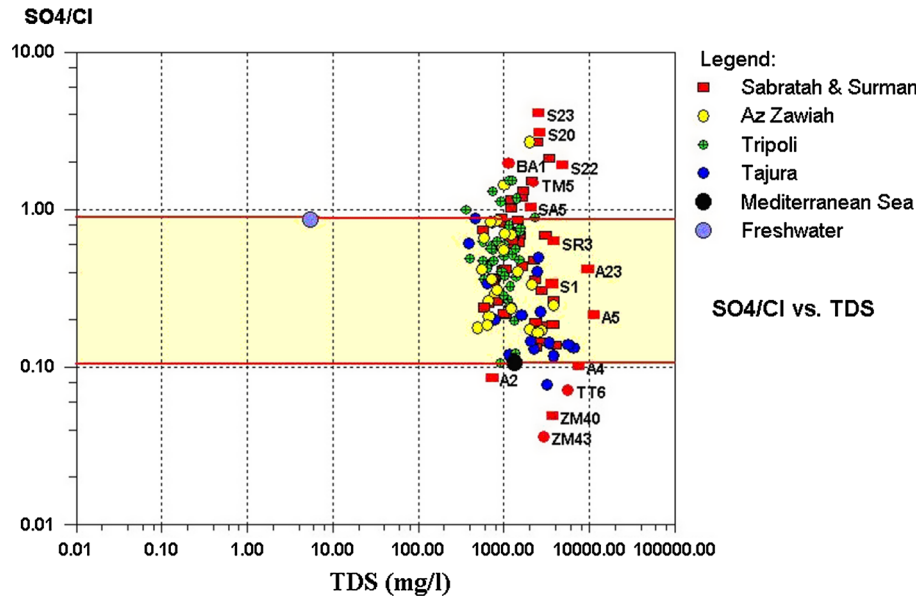

Fig. 10 Molar ratio of SO_4^{2-}/Cl^- versus TDS concentrations

(0.82 TJ17). Most of the analyzed samples are plotted between the ratio of 0.1 and 1.0, indicating mixing of the water with the Mediterranean seawater end member having ratio of 0.103. Few samples with very high salinity are having SO_4^{2-}/Cl^- ratio less than the Mediterranean Sea; this can suggest sulfate reduction. The gypsum dissolution-affected waters show the highest SO_4^{2-}/Cl^- ratio. This has further been illustrated in Fig. 11, where SO_4^{2-} versus x-coordinate in the coastal area (from west to east using the x-coordinates) depicts the distribution of SO_4^{2-}. The effect of gypsum dissolution is clear in sample S22, where the concentration is more than 45 meq/l (2238 mg/l).

Conclusion

The overpumping for groundwater has contributed to the deterioration of the water quality by marine intrusion and upconing of the deep saline water. Cl^- and SO_4^{2-} are the major pollutants of the aquifer.

Great part of the observed high concentration of sulfate is coming from the effect of seawater intrusion. Another source of SO_4^{2-} is dissolution of gypsum from the upper aquifer's formation in the south of the study area. Furthermore, the scattered sebkha deposits, containing large amounts of gypsum, produce high SO_4^{2-} waters, and the

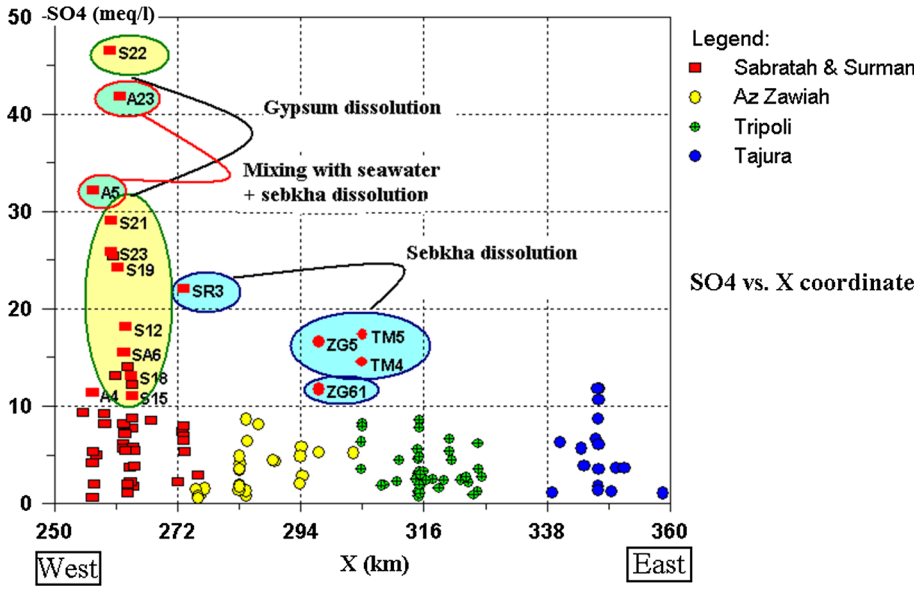

Fig. 11 SO_4^{2-} concentration (meq/l) versus x-coordinate

infiltration of these concentrated waters has affected many wells and has lead to the development of $CaSO_4$ water type for these wells. These processes were also studied by calculation of the saturation index with respect to gypsum, which increase with increasing Ca^{2+} and SO_4^{2-} in groundwater.

The hydrochemical interpretation also indicates that the dissolution of calcite, dolomite and/or Mg^{2+}-bearing calcite is an important process in most of the groundwaters. The saturation index shows mostly a tendency of precipitation of calcite and dolomite in the aquifer system due to lowering of CO_2 pressure at sampling.

Seawater intrusion is accompanied by other processes, which modify the hydrochemistry of the coastal aquifer. The most remarkable process is that of the inverse cation exchange, characteristic of the changes in the theoretical mixture of seawater–freshwater, which is carried out between clays and the aquifer water. This exchange consists in the release of Ca^{2+} and the adsorption of Na^{+}.

In the study area, the salinization phenomenon occurred in the downstream zones, where the NaCl and CaCl water types have mostly been developed. Somewhat less brackish water quality was identified in the upstream direction, in zones where pumping is less of a problem, indicating smaller seawater influence, whereby recharge from the south is limiting the degree of salinization.

Deterioration in groundwater quality in Jifarah Plain is mainly resulting from aquifer overexploitation; therefore, reducing the pumping rate is the first step to satisfy and recover the groundwater quality and quantity.

Acknowledgments This study was supported by the Libyan government through the Libyan Embassy in Brussels. Great thanks to the General Water Authority, Tripoli, Libya, the well owners and all who supported in the field campaigns. The authors want to thank three anonymous reviewers for their constructive criticism, which helped to improve the paper.

References

Alfarrah N (2011) Hydrogeological and hydrogeochemical investigation of the coastal area of Jifarah Plain, NW Libya. PhD thesis, Laboratory of Applied Geology and Hydrogeology, Ghent University, Belgium

Alfarrah N, Martens K, Walraevens K (2011) Hydrochemistry of the upper miocene-pliocene-quaternary aquifer complex of Jifarah plain, NW-Libya. Geologica Belgica 14(3–4):159–174

Alfarrah N, van Camp M, Walraevens K (2013) Deducing transmissivity from specific capacity in the heterogeneous upper aquifer system of Jifarah Plain, NW-Libya. J Afr Earth Sc 85:12–21

APHA (American Public Health Association) (1985) Standard methods for the examination of water and wastewater. In: Greenberg AE (APHA), Trussell RR (AWWA), Clesceri LS (WPCF) (eds).APHA, Washington, DC

Appelo CAJ (1994) Cation and proton exchange, pH variations, and carbonate reactions in a freshening aquifer. Water Resour Res. 30:2793–2805

Appelo CAJ, Postma D (1993) Geochemistry, groundwater and pollution: Rotterdam, Netherlands, and Brookfield, Vermont, A. A. Balkema

Bencini A, Pranzini G (1992) The salinization of groundwater in Grosseto Plain (Tus-cany). In: Custodio E, Galofré A (eds) Study and modelling of saltwater intrusion into aquifers. Proceedings of 12th SWIM 92, Barcelona, pp 161–175. Barcelona: CIMNE. 1993, pp 229–243

Bosch X, Custodio E (1992) Dissolution processes in the freshwater-saltwater mixing zone in carbonate sediments: the Cala Jostell area (Vandell6 s, Tarragona). Book

Chaouni Alia A, EL Halimi N, Walraevens K, Beeuwsaert E, De Breuck W (1997) Investigation de la salinisation de la plaine de Bou-Areg (Maroc nord-oriental). In: Proceedings of reports international association of hydrological sciences, freshwater contamination, vol 243, pp 211–220

Coetsiers M, Walraevens K (2006) Chemical characterization of the Neogene Aquifer, Belgium. Hydrogeol J 14:1556–1568

Coetsiers M, Walraevens K (2009) A new correction model for ^{14}C ages in aquifers with complex geochemistry—application to the Neogene Aquifer, Belgium. Appl Geochem 24:768–776

Coetsiers M, Blaser P, Martens K, Walraevens K (2009) Natural background levels and threshold values for groundwater in fluvial Pleistocene and Tertiary marine aquifers in Flanders, Belgium. Environ Geol 57:1155–1168

Da'as A, Walraevens K (2010) Groundwater salinity in Jericho Area, West Bank, Palestine. In: Proceedings of SWIM-21 salt water intrusion meeting, Ponta Delgada, San Miguel, Azores, Portuga, pp 28–31

Da'As A, Walraevens K (2013) Hydrogeochemical investigation of groundwater in Jericho area in the Jordan Valley, West Bank, Palestine. J Afr Earth Sc 82:15–32

Dixon W, Chiwell B (1992) The use of hydrochemical sections to identify recharge areas and saline intrusions in alluvial aquifers, Southeast Queensland, Australia. J Hydrogeol J 135:259–274

Fidelibus MD, Tulipano L (1996) Regional flow of intruding seawater in the carbonate aquifers of Apulia (Southern Italy). 14th SWIM, Malmö, Sweden, Rapporter och meddelanden, Geological Survey of Sweden, Uppsala

Fidelibus MD, Giménez E, Morell I, Tulipano L (1993) Salinization processes in the Castellon Plain aquifer (Spain). In: Custodio E, Galofré A (eds) Study and modelling of saltwater intrusion into aquifers. Centro Internacional de Métodos Numéricos en Ingeniería, Barcelona

Giménez E, Morell I (1997) Hydrogeochemical analysis of salinization processes in the coastal aquifer of Oropesa (Castellon, Spain). Environ Geol 29:118–131

Jeen SK, Kim JM, Ko KS, Yum B, Chang HW (2001) Hydrogeochemical characteristics of groundwater in a mid-western coastal aquifer system, Korea. Geosci J 5:339–348

Jones BF, Vengosh A, Rosenthal E, Yechieli Y (1999) Geochemical investigation of groundwater quality. Seawater intrusion in coastal aquifers-concepts, methods and practices. Kluwer, Netherlands, pp 51–71

Kreitler CW, Richter BC (1993) Geochemical techniques for identifying sources of groundwater salinization. C.K. Smoley, Boca Raton, Florida

LIRC (Libyan Industrial Research Centre) (1995) Geological card of Jifarah Plain, 2end edn. Tajura, Libya

Magaritz M, Luzier JE (1985) Water–rock interactions and seawater–freshwater mixing effects in the coastal dune aquifer, Coos Bay, Oregon. Appl Geochem 49:2515–2525

Masciopinto C (2006) Simulation of coastal groundwater remediation: the case of Nardò fractured aquifer in Southern Italy. Environ Model Softw 21:85–97

Masciopinto C, Barbieri G, Benedini M (1999) A large scale study for drinking water requirements in the Po basin (Italy). Water International. 24(3):211–220

Mjemah IC, van Camp M, Walraevens K (2009) Groundwater exploitation and hydraulic parameter estimation for a Quaternary aquifer in Dar-es-Salaam, Tanzania. J Afr Earth Sci 55(3–4):134–146

Morell I, Giménez E, Esteller MV (1996) Application of principal components analysis to the study of salinization on the Castellon Plain (Spain). Geosciences. 177:161–171

Mtoni YE, Mjemah IC, Msindai K, van Camp M, Walraevens K (2012) Saltwater intrusion in the quaternary aquifer of the Dar es Salaam region, Tanzania. Geologica Belgica. 15(1–2):16–25

Mtoni YE, Mjemah IC, Bakundukize C, van Camp M, Walraevens K (2013) Saltwater intrusion and nitrate pollution in the coastal aquifer of Dar es Salaam, Tanzania. Environ Earth Sci 70(3):1091–1111

Nadler A, Magaritz M, Mazor E (1981) Chemical reactions of seawater with rocks and freshwater experimental and field observations on brackish waters in Israel. Appl Geochem 44:879–886

Park CH, Aral MM (2004) A multi-objective optimisation of pumping rates and well placement in coastal aquifers. J Hydrol 290:80–99

Pulido-Leboeuf P (2004) Seawater intrusion and associated processes in a small coastal complex aquifer (Castell de Ferro, Spain). Appl Geochem 19:1517–1527

Stuyfzand PJ (1986) A new hydrogeochemical classification of water types: principles and application to the coastal dunes aquifer system of the Netherlands. In: Proceedings 9th SWIM, Delft (The Netherlands), pp 641–656

Stuyfzand PJ (1992) Behaviour of major and trace constituents in fresh and salt intrusion waters, in the western Netherlands. In: Custodio E, Galofré A (eds) Study and modelling of salt water intrusion into aquifers. Proceedings of the 12th salt water intrusion meeting, Barcelona. CIHS-CIMNE, Barcelona, pp 143–160

Stuyfzand PJ (1993) Hydrochemistry and hydrology of the coastal dune area of the Western Netherlands. PhD dissertation, Free University (VU), Amsterdam. 90-74741-01-0

Stuyfzand PJ (1999) Patterns in groundwater chemistry resulting from groundwater flow. Hydrogeol J 7:15–27

Sukhija BS, Varma VN, Nagabhushanam P, Reddy DV (1996) Differentiation of paleomarine and modern intruded salinities in coastal groundwaters (of Karaikal and Tanjavur, India) based on inorganic chemistry, organic biomarker fingerprints and radiocarbon dating. J Hydrol 174:173–201

Todd DK (1980) Groundwater hydrology, 2nd edn. John Wiley, New York, p 535

van Camp M, Walraevens K (2009) Recovery scenarios for deep over-exploited aquifers with limited recharge: methodology and application to an aquifer in Belgium. Environ Geol 56(8):1505–1516

van Camp M, Radfar M, Walraevens K (2010) Assessment of groundwater storage depletion by overexploitation using simple indicators in an irrigated closed aquifer basin in Iran. Agric Water Manag 97(11):1876–1886

van Camp M, Radfar M, Martens K, Walraevens K (2012) Analysis of the groundwater resource decline in an intramountain aquifer system in Central Iran. Geologica Belgica 15(3):176–180

van Camp M, Mjemah IC, Al Farrah N, Walraevens K (2013) Modeling approaches and strategies for data-scarce aquifers: example of the Dar es Salaam aquifer in Tanzania. Hydrogeol J 21:341–356

van Camp M, Mtoni YE, Mjemah IC, Bakundukize C, Walraevens K (2014) Investigating seawater intrusion due to groundwater pumping with schematic model simulations : the example of the Dar Es Salaam coastal aquifer in Tanzania. J Afr Earth Sc 96:71–78

Vengosh A, Starinsky A, Melloul A, Fink M, Erlich S (1991) Salinization of the coastal aquifer water by Ca-chloride solutions at the interface zone, along the coastal plain of Israel. Hydrological Service, Jerusalem

Walraevens K (1987) Hydrogeology and hydrochemistry of the Ledo-Paniselian in Eastern and Western Flanders (in Dutch). +fig. +annexes. PhD dissertation, Ghent University

Walraevens K, Van Camp M (2005) Advances in understanding natural groundwater quality controls in coastal aquifers, 18 SWIM. Cartagena 2004, Spain, pp 451–460

Walraevens K, Boughriba M, De Breuck W (1993a). Groundwater quality evolution in the Black-Sluice Polder area around Assenede (Belgium). In: Custodio E, Galofre A (eds) Study and modelling of saltwater intrusion into aquifers. Centro Internacional de Métodos Numéricos en Ingenieria, Barcelona, pp 121–142

Walraevens K, Lebbe L, Van Camp M, Angius G, Serra M, Vacca A, Massidda R, Debreuck W (1993b) Study and modelling of saltwater intrusion into aquifers, pp 407–420

Walraevens K, Lebbe L, de Ceukelaire M, van Houtte E, de Breuck W, Marras F (1994) Influence on groundwater quality of the Paleozoic Brabant Massif in Belgium due to overexploitation. Int Assoc Hydrol Sci 220:461–470

Walraevens K, Cardenal-Escarcena J, van Camp M (2007) Reaction transport modelling of a freshening aquifer (Tertiary Ledo-Paniselian Aquifer, Flanders, Belgium). Appl Geochem 22:289–305

Walraevens K, Mjemah IC, Mtoni Y, van Camp M (2015) Sources of salinity and urban pollution in the Quaternary sand aquifers of Dar es Salaam, Tanzania. J Afr Earth Sc 102:149–165